MATHEMATICAL BIOSCIENCES
AND ENGINEERING
Volume **12**, Number **4**, August **2015**

doi:10.3934/mbe.2015.12.699

pp. **699–715**

BIFURCATION ANALYSIS AND TRANSIENT SPATIO-TEMPORAL DYNAMICS FOR A DIFFUSIVE PLANT-HERBIVORE SYSTEM WITH DIRICHLET BOUNDARY CONDITIONS

Lin Wang, James Watmough and Fang Yu

Department of Mathematics and Statistics
University of New Brunswick
Fredericton, New Brunswick, E3B 5A3, Canada

Abstract. In this paper, we study a diffusive plant-herbivore system with homogeneous and nonhomogeneous Dirichlet boundary conditions. Stability of spatially homogeneous steady states is established. We also derive conditions ensuring the occurrence of Hopf bifurcation and steady state bifurcation. Interesting transient spatio-temporal behaviors including oscillations in one or both of space and time are observed through numerical simulations.

1. **Introduction.**

In this paper we consider the following diffusive plant-herbivore system

$$\begin{aligned} \frac{\partial u}{\partial t} &= d_1 u_{xx} + ru(1-u) - \frac{uv}{1+\beta u}, \quad x \in \Omega,\ t > 0, \\ \frac{\partial v}{\partial t} &= d_2 v_{xx} + \frac{uv}{1+\sigma u} - \kappa v, \qquad x \in \Omega,\ t > 0 \end{aligned} \tag{1}$$

with Dirichlet boundary conditions

$$u(t,x)|_{x\in\partial\Omega} = v(t,x)|_{x\in\partial\Omega} = 0, t > 0 \tag{2}$$

or

$$u(t,x)|_{x\in\partial\Omega} = u_1, v(t,x)|_{x\in\partial\Omega} = v_1,\ t > 0 \tag{3}$$

where

$$u_1 = \frac{\kappa}{1-\kappa\sigma},\ v_1 = \frac{r(1-\kappa\sigma-\kappa)(1-\kappa\sigma+\kappa\beta)}{(1-\kappa\sigma)^2}. \tag{4}$$

Here $u(x,t)$ and $v(x,t)$ represent the population densities of the plant and herbivore location $x \in \Omega$ (For simplicity, we take $\Omega = (0,\pi)$) and time $t > 0$, respectively; d_1 and d_2 are the diffusion coefficients; r is the intrinsic growth rate of the plant in the absence of herbivores; κ is the death rate of the herbivore; The positive constants β and σ are the scaling parameters of functional response (characterized by the function $\frac{u}{1+\beta u}$) and numerical response (characterized by the function $\frac{u}{1+\sigma u}$), respectively.

If $\beta = \sigma$, then (7) reduces to the diffusive predator-prey model in which numerical response is assumed to be proportional to functional response, which has been

2010 *Mathematics Subject Classification.* Primary: 35B32, 35B35; Secondary: 92B05.

Key words and phrases. Plant-herbivore interaction, diffusion, Hopf bifurcation, steady state bifurcation, transient dynamics.

The first two authors were partially supported by NSERC of Canada.

extensively studied in the literature. See, for example, [1, 2, 4, 5, 9, 12] and the references therein.

In this paper, we do not necessarily assume that $\beta = \sigma$ since in plant-herbivore interaction, the numerical response is generally not proportional to the functional response. As pointed out in [8] that at high plant density, herbivore may cut off, discard without consuming them so that the herbivore reproduction is not a linear function of its consumption. Also assuming $\beta \neq \sigma$ may have applications in plant defense [6, 10].

The rest of this paper is organized as follows. Section 2 is devoted to the dynamics of System (1) with boundary condition (2). In Section 3, we study the linear stability and instability of the positive spatially homogeneous steady state of System (1) with the boundary condition (3) and investigate the occurrence of Hopf bifurcation and steady state bifurcation. Transient spatio-temporal patterns induced by Hopf and steady state bifurcations are explored in Section 4. We summarize and discuss our work in Section 5.

Throughout this paper, for convenience, we introduce the notations: $\mathbb{N}(a) = \{a, a+1, a+2, \cdots\}$, $\mathbb{N}(a,b) = \{a, a+1, \cdots, b-1, b\}$ for $a < b$, $\mathbb{N}(a,a) = \{a\}$, $\mathbb{N}(a,b) = \emptyset$ if $b < a$, $\lfloor s \rfloor$ is the largest integer that is less than or equal to s.

2. System (1) with homogeneous Dirichlet boundary condition.

In this section, we consider System (1) with homogeneous Dirichlet boundary condition (2), i.e., we consider the following diffusive system:

$$\begin{aligned} \frac{\partial u}{\partial t} &= d_1 u_{xx} + ru(1-u) - \frac{uv}{1+\beta u}, && x \in (0,\pi),\ t > 0, \\ \frac{\partial v}{\partial t} &= d_2 v_{xx} + \frac{uv}{1+\sigma u} - \kappa v, && x \in (0,\pi),\ t > 0, \\ u(t,0) &= u(t,\pi) = v(t,0) = v(t,\pi) = 0, && t > 0. \end{aligned} \tag{5}$$

For System (5), the only spatially homogeneous steady state is $E_0 = (0,0)$. Our next result shows that E_0 is indeed the only nonnegative steady state of System (5) if $r < d_1$ and there will be another nonnegative steady state if $r > d_1$.

Theorem 2.1. *Consider System (5). If $r < d_1$, then E_0 is the only nonnegative steady state, which is stable. If $r > d_1$, then E_0 is unstable and there exists an additional nonnegative steady state $(u_0, 0)$ with $u_0(x) > 0$ for $x \in (0,\pi)$.*

Proof. Linearization of (5) at E_0 gives the characteristic equation:

$$z_n^2 - T_n^0 z_n + D_n^0 = 0, \quad n = 1,2,3,\ldots, \tag{6}$$

where

$$T_n^0 := r - \kappa - (d_1 + d_2)n^2$$

and

$$D_n^0 := (d_1 n^2 - r)(\kappa + d_2 n^2).$$

If $r < d_1$, then $D_n^0 > D_1 > 0$ and $T_n^0 < T_1 < 0$ for $n = 1, 2, \ldots$. This implies that all eigenvalues of the characteristic equation have negative real parts for each n and hence E_0 is stable. If $r > d_1$, then $D_1^0 < 0$, which implies that for $n = 1$, there exists one positive real eigenvalue. Therefore, E_0 is unstable if $r > d_1$.

Theorem 1.B in [9] states that if $M(0,0) \leq \lambda_1$, then $(0,0)$ is the only nonnegative solution. Here $M = r(1-u) - \frac{v}{1+\beta u}$ and λ_1 is the first eigenvalue of the operator

$-\frac{\partial^2}{\partial x^2}$. That is, $M(0,0) = r$, and $\lambda_1 = d_1$. Hence E_0 is the unique nonnegative steady state of (5) if $r < d_1$.

By [9, Lemma 1.1], if $r > d_1$, then System (5) admits a nonnegative steady state $(u_0(x), 0)$, where $u_0(x)$ is the unique positive solution of the equation $0 = d_1 u_{xx} + ru(1-u)$ with $u(t,0) = u(t,\pi) = 0$. □

Theorem 2.2. *For System (5), Hopf bifurcation can never occur at E_0. Furthermore, a steady state bifurcation occurs provided $\frac{r}{d_1} = n^2$ for some $n \geq 1$.*

Proof. It follows from the definitions of T_n^0 and D_n^0 that $D_n^0 < 0$ whenever $T_n^0 = 0$. This implies that the condition for Hopf bifurcation can never be satisfied. Thus Hopf bifurcation can never occur at E_0. On the other hand, if $D_n^0 = 0$ for some positive integer n, then $T_n^0 \neq 0$. This indicates that steady state bifurcation occurs at E_0 if $\dfrac{r}{d_1} = n^2$ for some $n \geq 1$. □

3. **System (1) with nonhomogeneous boundary condition.** In this section we consider System (1) with the boundary condition (3), that is, we consider the following diffusive system:

$$\begin{aligned} \frac{\partial u}{\partial t} &= d_1 u_{xx} + ru(1-u) - \frac{uv}{1+\beta u}, && x \in (0,\pi),\ t > 0, \\ \frac{\partial v}{\partial t} &= d_2 v_{xx} + \frac{uv}{1+\sigma u} - \kappa v, && x \in (0,\pi),\ t > 0, \\ u(t,0) &= u(t,\pi) = u_1, \quad v(t,0) = v(t,\pi) = v_1, && t > 0, \end{aligned} \tag{7}$$

where u_1 and v_1 are given in (4). If $\sigma < \sigma_0 = \frac{1}{k} - 1$, then System (7) has a unique spatially homogeneous steady state $E^* = (u_1, v_1)$. Next we consider the linear stability and instability of the steady state E^*.

The linearized operator of System (7) at the steady state (u_1, v_1) is given by

$$\bar{\mathcal{L}} \begin{pmatrix} \bar{\phi} \\ \bar{\psi} \end{pmatrix} = \bar{D} \begin{pmatrix} \bar{\phi}_{xx} \\ \bar{\psi}_{xx} \end{pmatrix} + J \begin{pmatrix} \bar{\phi} \\ \bar{\psi} \end{pmatrix}, \tag{8}$$

where

$$\bar{D} = \begin{pmatrix} d_1 & 0 \\ 0 & d_2 \end{pmatrix}, \ J = \begin{pmatrix} r - 2ru_1 - \dfrac{v_1}{(1+\beta u_1)^2} & -\dfrac{u_1}{1+\beta u_1} \\ \dfrac{v_1}{(1+\sigma u_1)^2} & \dfrac{u_1}{1+\sigma u_1} - \kappa \end{pmatrix}.$$

The characteristic equation of the linear operator $\bar{\mathcal{L}}$ is

$$\bar{\mathcal{L}} \begin{pmatrix} \bar{\phi} \\ \bar{\psi} \end{pmatrix} = \lambda \begin{pmatrix} \bar{\phi} \\ \bar{\psi} \end{pmatrix}, \tag{9}$$

where

$$\begin{pmatrix} \bar{\phi} \\ \bar{\psi} \end{pmatrix} = \sum_{n=0}^{\infty} \begin{pmatrix} \bar{e}_n \\ \bar{l}_n \end{pmatrix} \sin(nx) \tag{10}$$

and $\bar{e}_n, \bar{l}_n$ are coefficients.

The linear stability of the steady state E^* of System (7) is then determined by the eigenvalues of the characteristic equation:

$$z_n^2 - T_n z_n + D_n = 0, n = 1, 2, 3, \ldots, \tag{11}$$

where

$$T_n := T(\beta) - (d_1 + d_2)n^2, \tag{12}$$

$$D_n := d_1 d_2 n^4 - d_2 T(\beta) n^2 + D \tag{13}$$

with $T(\beta) = \dfrac{r\kappa\,(\beta - 2\beta\kappa - 1 + \kappa(1-\beta)\sigma)}{(1-\sigma\kappa)(1+\beta\kappa-\sigma\kappa)}$ and $D = r\kappa(1-\kappa-\sigma\kappa) > 0$. If $T_n < 0$ and $D_n > 0$ for all $n = 1, 2, 3, \ldots$, then E^* is stable.

Lemma 3.1. *If* $0 < \beta \le 1$ *or* $\beta > 1$ *and* $0 < \sigma < \sigma^* < \sigma_0$, *where* $\sigma^* = \frac{1}{\kappa} - \dfrac{2\beta}{\beta - 1}$, *then* E^* *is locally asymptotically stable.*

Proof. Under the given conditions, E^* is the unique positive equilibrium of the corresponding local system, which can be shown to be locally asymptotically stable. That is, we have $T(\beta) < 0$. Thus, from (12) and (13), we have $T_n < 0$ and $D_n > 0$ for all $n = 1, 2, 3, \ldots$. This shows that the steady state E^* of System (7) is locally asymptotically stable. □

Remark 1. Lemma 3.1 shows that the diffusion in System (7) does not destabilize a rather stable local system. Indeed, as we will show later, it is interesting to note that the steady state E^* of System 7 may be stable even if the local system is unstable when the diffusion coefficients are sufficient large (see Figures 3 and 4), which indicates that the diffusion has a stabilizing effect.

To further study the stability and instability of E^*, we first establish several lemmas.

Lemma 3.2. *If*

$$\frac{r(1-2\kappa-\kappa\sigma)}{1-\kappa\sigma} \le 2\sqrt{\frac{d_1 D}{d_2}}, \tag{14}$$

then $D_n > 0$ *for any* $n \in \mathbb{N}(1)$.

Proof. Note $D_n = d_1 d_2 n^4 - d_2 T(\beta) n^2 + D$ can be regarded as a quadratic polynomial of n^2 with the discriminant

$$\delta(D_n) := d_2^2 T^2(\beta) - 4 d_1 d_2 D.$$

Since $T'(\beta) = \frac{r\kappa(1-\kappa\sigma-\kappa)}{(1-\kappa\sigma+\beta\kappa)^2} > 0$ and

$$T(\beta) < \lim_{\beta\to\infty} T(\beta) = \frac{r(1-2\kappa-\kappa\sigma)}{1-\kappa\sigma},$$

condition (14) implies that $\delta(D_n) < 0$. Thus $D_n > 0$ for any $n = 1, 2, \ldots$. □

Next we assume that

$$\frac{r(1-2\kappa-\kappa\sigma)}{1-\kappa\sigma} > 2\sqrt{\frac{d_1 D}{d_2}}. \tag{15}$$

Solving $D_n = 0$ for β gives the critical point of neutral stability:

$$\beta = \beta_{1c}(n) = \frac{(1-\kappa\sigma)(r\kappa d_2 n^2 + (1-\kappa\sigma)(D + d_1 d_2 n^4))}{\kappa[r(1-2\kappa-\kappa\sigma)d_2 n^2 - (1-\kappa\sigma)(D + d_1 d_2 n^4)]} \tag{16}$$

for $n \in \mathbb{N}(\lfloor n_- \rfloor + 1, \lfloor n_+ \rfloor)$, where

$$n_\pm = \sqrt{\frac{r(1-2\kappa-\kappa\sigma)d_2 \pm \sqrt{\Delta}}{2(1-\kappa\sigma)d_1 d_2}} \tag{17}$$

with $\underline{\Delta} = (rd_2(1-2\kappa-\kappa\sigma))^2 - 4(1-\kappa\sigma)^2 d_1 d_2 D > 0$ (By (15)). Since

$$\frac{d\beta_{1c}(n)}{dn} = \frac{2rd_2 n(1-\kappa\sigma)^2(1-\kappa-\kappa\sigma)(d_1d_2n^4 - r\kappa + r\kappa^2 + r\kappa^2\sigma)}{k[r(1-2\kappa-\kappa\sigma)d_2n^2 - (1-\kappa\sigma)(D+d_1d_2n^4)]^2},$$

$\beta_{1c}(n)$ is decreasing with respect to n for $n < \bar{n}$ and increasing for $n > \bar{n}$, where $\bar{n} = \sqrt[4]{\frac{r\kappa(1-\kappa-\kappa\sigma)}{d_1d_2}}$ if it is an integer or one of the two closest integers. At this critical wave number $\bar{n}$,

$$\beta_{1c}(\bar{n}) = \min\{\beta_{1c}(n), n \in \mathbb{N}(\lfloor n_-\rfloor + 1, \lfloor n_+\rfloor)\}.$$

Lemma 3.3. *If*

$$0 < \beta < \beta_{1c}(\bar{n}), \tag{18}$$

then $D_n > 0$ for all $n \in \mathbb{N}(1)$. Moreover, if

$$\beta > \beta_{1c}(\bar{n}), \tag{19}$$

then there exists at least one n such that $D_n < 0$.

Proof. Note that $T'(\beta) > 0$ and

$$\frac{\partial D_n}{\partial \beta} = -d_2 n^2 T'(\beta) < 0. \tag{20}$$

Therefore, for $n \in \mathbb{N}(\lfloor n_-\rfloor + 1, \lfloor n_+\rfloor)$,

$$\begin{cases} D_n < 0 & \text{if } \beta > \beta_{1c}(n), \\ D_n > 0 & \text{if } 0 < \beta < \beta_{1c}(n), \end{cases} \tag{21}$$

and $D_n > 0$ for all n when $0 < \beta < \beta_{1c}(\bar{n})$. □

Remark 2. The above lemma shows that condition (19) implies that the characteristic equation admits a positive real root resulting in the instability of E^*.

Lemma 3.4. *If*

$$\frac{r(1-2k-k\sigma)}{(1-k\sigma)} \le d_1 + d_2, \tag{22}$$

then $T_n < 0$ for any $n \in \mathbb{N}(1)$.

Proof. The proof follows directly from the expression of T_n. □

If

$$\frac{r(1-2k-k\sigma)}{(1-k\sigma)} > d_1 + d_2, \tag{23}$$

then solving $T_n = 0$ for β yields the critical point of marginal stability

$$\beta = \beta_{2c}(n) = \frac{(1-\sigma\kappa)\left(r\kappa + (d_1+d_2)(1-\sigma\kappa)n^2\right)}{\kappa\left[r(1-2\kappa-\sigma\kappa) - (d_1+d_2)(1-\sigma\kappa)n^2\right]} \tag{24}$$

for $n \in \mathbb{N}(1, N_H)$, where

$$N_H = \left\lfloor \sqrt{\frac{r(1-2\kappa-\kappa\sigma)}{(1-\kappa\sigma)(d_1+d_2)}} \right\rfloor. \tag{25}$$

Lemma 3.5. *If*

$$0 < \beta < \beta_{2c}(1), \tag{26}$$

then $T_n < 0$ for all $n \in \mathbb{N}(1)$. If

$$\beta > \beta_{2c}(1), \tag{27}$$

there exists at least one $n \in \mathbb{N}(1, N_H)$ such that $T_n > 0$.

Proof. It is straightforward to verify that T_n is increasing in β and decreasing in n. Therefore, for $n \in \mathbb{N}(1, N_H)$,

$$\begin{cases} T_n > 0 & \text{if } \beta > \beta_{2c}(n), \\ T_n < 0 & \text{if } 0 < \beta < \beta_{2c}(n). \end{cases} \tag{28}$$

This shows that if (26) holds, then $T_n < T_1 < 0$ for any $n \in \mathbb{N}(2)$ and this gives the first statement. If (27) holds, then $T_1 > 0$ and there exists at least one $n \in \mathbb{N}(1, N_H)$ such that $T_n > 0$. □

We now present our result on the stability of E^*.

Theorem 3.6. *Consider System* (7) *with* $\sigma < \sigma_0$*. If* $0 < \beta \le 1$ *or* $\beta > 1$ *and* $0 < \sigma < \sigma^* < \sigma_0$ *or the following two conditions are satisfied:*

(i) either (14) or (15) and (18),
(ii) either (22) or (23) and (26),

then the unique spatially homogeneous steady state E^* *is linearly stable.*

Proof. It follows from Lemmas 3.2 and 3.3 that $D_n > 0$ for $n \in \mathbb{N}(1)$ if condition (i) is satisfied. If condition (ii) is satisfied, then by Lemmas 3.4 and 3.5, we have $T_n < 0$ for $n \in \mathbb{N}(1)$. Thus the stability of E^* follows. □

Our next result gives conditions under which the steady state E^* becomes unstable as a positive real eigenvalue appears.

Theorem 3.7. *If (15) and (19) hold, then the characteristic equation has positive real eigenvalues and* E^* *is a saddle point.*

Proof. If (15) and (19) hold, then by Lemma 3.3, we know that $D_n < 0$ for some $n \in \mathbb{N}(1)$. Thus for this n, the characteristic equation has a positive real root and thus E^* is a saddle point. □

We next present an instability result of E^* in which the characteristic equation has complex eigenvalues for some $n \in \mathbb{N}(1)$ and thus E^* is an unstable spiral. To this end, we define several terms as below:

$$\beta_- = \frac{(1-\kappa\sigma)^2((d_1-d_2)n^2 - 2\sqrt{D}) + r\kappa(1-\kappa\sigma)}{r\kappa(1-2\kappa-\kappa\sigma) - \kappa(1-\kappa\sigma[(d_1-d_2)n^2 - 2\sqrt{D}])},$$

$$\beta_+ = \frac{(1-\kappa\sigma)^2((d_1-d_2)n^2 + 2\sqrt{D}) + r\kappa(1-\kappa\sigma)}{r\kappa(1-2\kappa-\kappa\sigma) - \kappa(1-\kappa\sigma[(d_1-d_2)n^2 + 2\sqrt{D}])},$$

$$\beta_* = \frac{1-\kappa\sigma}{1-2\kappa-\kappa\sigma},\ \hat{\beta} = \max\left(\beta_*, \beta_-, \beta_{2c}(n)\right)$$

and

$$\check{\beta} = \begin{cases} \beta_+ & \text{if (14) holds,} \\ \min(\beta_+, \beta_{1c}(n)) & \text{if (15) holds.} \end{cases}$$

Theorem 3.8. *If (23) and*

$$\beta \in (\hat{\beta}, \check{\beta}) \tag{29}$$

hold, then the characteristic equation admits complex eigenvalues with positive real parts for some $n \in \mathbb{N}(1)$ *and* E^* *is an unstable spiral.*

Proof. The homogeneous steady state E^* becomes unstable through complex eigenvalues of the characteristic equation (11) if $T_n > 0$, $D_n > 0$ and $T_n^2 < 4D_n$ for some $n \in \mathbb{N}(1)$. It follows from $T_n^2 < 4D_n$ that

$$T(\beta_-) := (d_1 - d_2)n^2 - 2\sqrt{D} < T(\beta) < (d_1 - d_2)n^2 + 2\sqrt{D} =: T(\beta_+),$$

which, together with the monotonicity of $T(\beta)$, derives that

$$\beta_- < \beta < \beta_+. \tag{30}$$

Note that $T(\beta) > 0$ requires

$$\beta > \beta_*. \tag{31}$$

Combining (23), (28), (30) and (31) and conditions for $D_n > 0$, we know that the homogeneous steady state E^* becomes unstable through complex eigenvalues of the characteristic equation for some $n \in \mathbb{N}(1)$ if (23) and (29) hold. □

Linear stability diagrams resulting from the above analysis are illustrated in Figure 1 with parameter values given by: $r = 8$, $\kappa = 0.08$, $\sigma = 5$, $d_1 = 0.008$, $d_2 = 0.08$. By Theorem 3.6, the spatially homogeneous steady state E^* is linearly stable if $\beta \in (0, 1.50)$ and is unstable if $\beta > 1.50$.

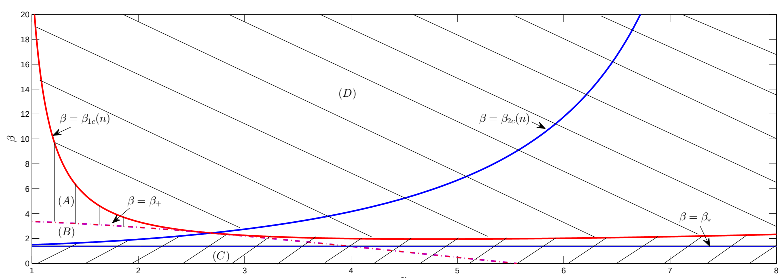

FIGURE 1. Linear stability diagrams in the $\beta - n$ space. Region (A): E^* is an unstable node; Region (B): E^* is an unstable spiral with complex eigenvalues; Region (C): E^* is stable; Region (D): E^* is a saddle point with $D_n < 0$. Parameter values used: $r = 8$, $\kappa = 0.08$, $\sigma = 5$, $d_1 = 0.008$, $d_2 = 0.08$.

3.1. **Hopf bifurcation and steady state bifurcation.** In this section we regard β as a bifurcation parameter to explore the occurrence of Hopf bifurcation and steady state bifurcation at the homogeneous steady state E^*. We have the following result on Hopf bifurcation and steady state bifurcation of System 7. It follows from the general Hopf bifurcation theory [7] that if for a positive integer $n \in \mathbb{N}(1)$, there exists a critical value β_n^H such that the characteristic equation (11) has a pair of simple purely imaginary eigenvalues $z_n = \pm i\omega(\beta_n^H)$ satisfying the transversality condition $\frac{dRe(z_n)}{d\beta}|_{\beta=\beta_n^H} \neq 0$, then $\beta = \beta_n^H$ is a Hopf bifurcation value. Applying the abstract bifurcation theorem of Crandall and Rabinowitz [3], we know that a steady state bifurcation occurs if there exists a critical value β_n^S for some integer $n \in \mathbb{N}(1)$ at which

$$D_n = 0, T_n \neq 0, D_j \neq 0, j \neq n \tag{32}$$

and

$$\left.\frac{\partial D_n}{\partial \beta}\right|_{\beta=\beta_n^S} \neq 0. \tag{33}$$

Theorem 3.9. *Assume $\sigma < \sigma_0$. For System (7) with $\beta_{1c}(n), \beta_{2c}(n), N_h, n_\pm$ defined in (16), (24), (25) and (17), respectively, if $\frac{r(1-2k-k\sigma)}{(1-k\sigma)} > d_1 + d_2$, then Hopf bifurcation occurs at β_n^H with*

$$\beta_n^H \in \{\beta_{2c}(j) : D_j > 0, j \in \mathbb{N}(1, N_h)\}. \tag{34}$$

Proof. We first prove that there are finite number of Hopf bifurcation values. Note that $Re(z_n) = \frac{T_n}{2}$ and $\frac{dRe(z_n)}{d\beta} = \frac{1}{2}\frac{dT_n}{d\beta} = \frac{1}{2}T'(\beta) > 0$. Thus the transversality condition always holds. If (23) holds, then it follows from (24) that there are finite number of critical points $\beta_n^H = \beta_{2c}(n)$ at which $T_n(\beta_n^H) = 0$ and $T_j(\beta_n^H) \neq 0$ for $j \neq n$, where $n, j \in \mathbb{N}(1, N_h)$. If further for the same n, $D_n(\beta_n^H) > 0$, i.e., $\beta_{2c}(n) < \beta_{1c}(n)$, then such a β_n^H is a Hopf bifurcation value. These critical points can be easily located geometrically from the plots of $(\beta_{1c}(n), n)$ and $(\beta_{2c}(n), n)$ (see Figures 2 and 9). □

Theorem 3.10. *Assume $\sigma < \sigma_0$. For System (7) with $\beta_{1c}(n), \beta_{2c}(n), N_h, n_\pm$ defined in (16), (24), (25) and (17), respectively, if $\frac{r(1-2\kappa-\kappa\sigma)}{1-\kappa\sigma} > 2\sqrt{\frac{d_1 D}{d_2}}$, then steady state bifurcation occurs at β_n^S with*

$$\beta_n^S \in \{\beta_{1c}(j) : T_j \neq 0, j \in \mathbb{N}(\lfloor n_- \rfloor + 1, \lfloor n_+ \rfloor)\}. \tag{35}$$

Proof. We prove that there are finite number of steady state bifurcation values. The transversality condition (33) follows from (20). Note that $D_n = 0$ is possible only when (15) holds. Under (15), by (16), there are finite number of critical points $\beta_n^S = \beta_{1c}(n)$ at which $D_n = 0, D_j \neq 0$ for $j \neq n$, $n, j \in \mathbb{N}(\lfloor n_- \rfloor + 1, \lfloor n_+ \rfloor)$. These critical values β_n^S are steady state bifurcation values provided $\beta_n^S \neq \beta_{2c}(n)$. □

Remark 3. There are three possible scenarios: (i) there exist some Hopf bifurcation values and also some steady state bifurcation values; (ii) there are Hopf bifurcation values but no steady state bifurcation values; (iii) there are steady state bifurcation values but no Hopf bifurcation values. For example, (i) is possible if (15) and (23) hold; (ii) is possible if (14) and (23) hold; and (iii) occurs if (15) and (22) hold.

4. Transient spatio-temporal patterns induced by Hopf and steady state bifurcations.

In this section, we present some numerical simulations to illustrate our analytical results and explore those three possible scenarios mentioned in Remark 3. To this end, three sets of parameters were used: (i) $r = 8$, $\kappa = 0.08$, $\sigma = 5$, $d_1 = 0.008$, $d_2 = 0.08$; (ii) $r = 8$, $\kappa = 0.08$, $\sigma = 5$, $d_1 = 0.08$, $d_2 = 0.0008$; (iii) $r = 0.2$, $\kappa = 0.08$, $d_1 = 0.08$, $d_2 = 0.8$, $\sigma = 5$.

With parameter set (i), (15) and (23) hold, by Theorems 3.9 and 3.10, there are two Hopf bifurcation values $\beta_1^H \approx 1.50$ and $\beta_2^H \approx 1.93$ and 27 steady state bifurcation values $\{1.95, 1.99, 2.02, \cdots\}$. The determination of these critical values are demonstrated in Figure 2. Theorems 3.6, 3.9 and 3.10 show that the spatially homogeneous steady state E^* is stable if $\beta \in (0, 1.50)$ and if $\beta > 1.50$, then E^* becomes unstable and there are spatially nonhomogeneous periodic solutions bifurcating from E^* when β is near the Hopf bifurcation values and there are spatially nonhomogeneous steady states bifurcating from E^* when β is close to the steady state bifurcation values.

We take $\beta = 1.45$, which is smaller than the first Hopf bifurcation value $\beta_1^H = 1.50$, as shown in Figure 3, the spatially homogeneous steady state E^* is stable. Note that for this set of parameter values, the positive equilibrium E^* of the corresponding local system is unstable (see Figure 4). This confirms that diffusion

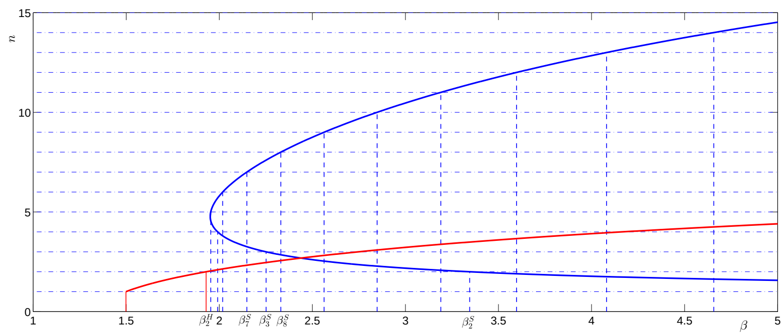

FIGURE 2. Determination of Hopf bifurcation values and steady state bifurcation values for System (7). Parameter values used: $r = 8$,$\kappa = 0.08$, $\sigma = 5$, $d_1 = 0.008$, $d_2 = 0.08$. Hopf bifurcation values are: $\beta_1^H = 1.5$, $\beta_2^H = 1.93$. Partial steady state bifurcation values are: $\beta_2^S = 3.35$, $\beta_3^S = 2.25$, $\beta_4^S = 1.99$, $\beta_5^S = 1.95$, $\beta_6^S = 2.02$, $\beta_7^S = 2.15$, $\beta_8^S = 2.33$.

can stabilize a rather unstable system. If we increase β to $\beta = 1.52$, which is near $\beta_1^H = 1.50$, as shown in Figures 5 and 6, the solution does not approach E^*, instead, a spatially non-homogeneous periodic solution appears and attracts the solutions of System (7).

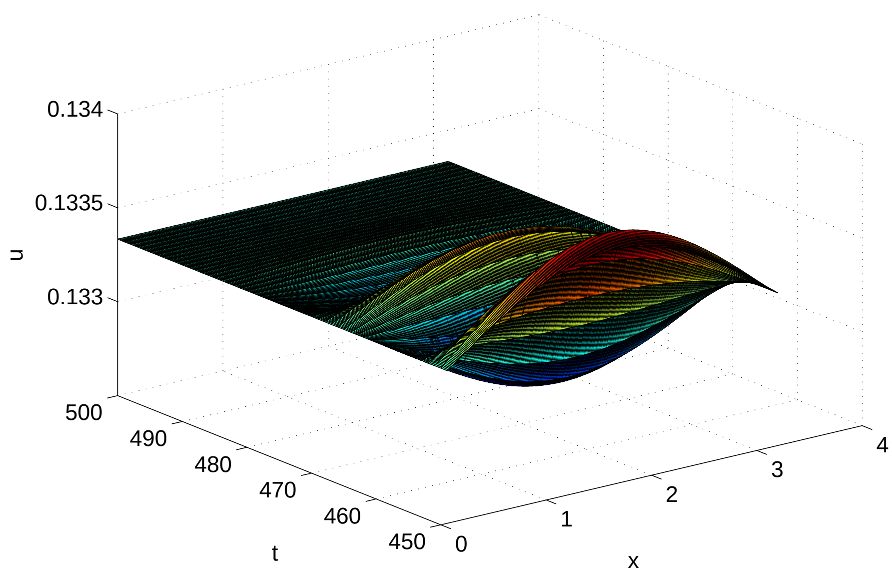

FIGURE 3. The $u-$component of a numerical solution of System (7) with parameter values: $r = 8$, $\kappa = 0.08$, $\sigma = 5$, $d_1 = 0.008$, $d_2 = 0.08$, $\beta = 1.45$ and initial condition: $u_0(x) = u_1 + 0.01\sin(x)$, $v_0(x) = v_1 + 0.2\sin(x)$. Since $\beta = 1.45 < \beta_1^H = 1.50$, E^* is stable.

We further increase the value of β to $\beta = 2$, which is now close to the steady state bifurcation value $\beta_4^S = 1.99$. Different from Figure 6, we can observe very

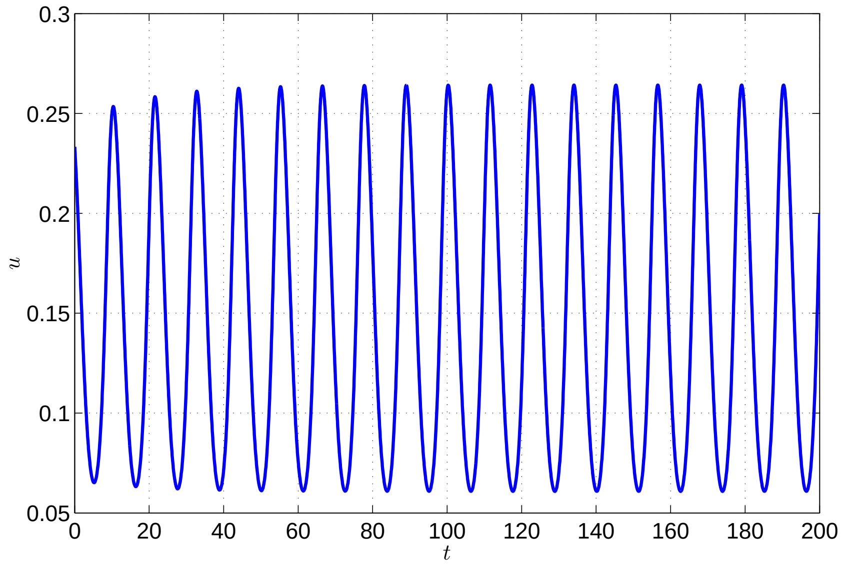

FIGURE 4. The $u-$component of a numerical solution of the corresponding local system with parameter values: $r = 8$, $\kappa = 0.08$, $\sigma = 5$, $d_1 = 0.008$, $d_2 = 0.08$, $\beta = 1.45$. The positive equilibrium E^* is unstable and the solution converges to a stable periodic solution.

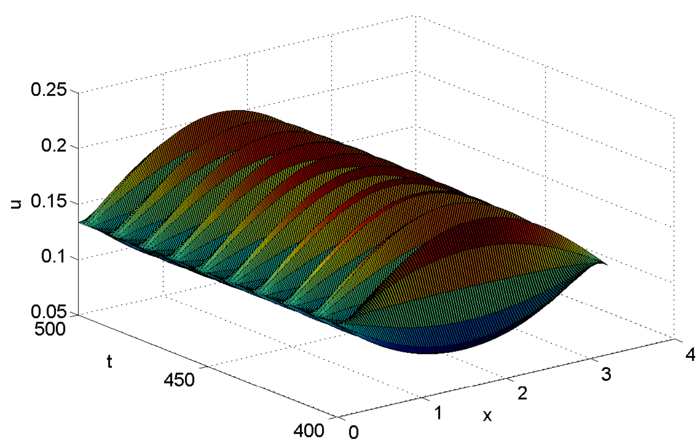

FIGURE 5. The $u-$component of a numerical solution of System (7) with parameter values: $r = 8$, $\kappa = 0.08$, $\sigma = 5$, $d_1 = 0.008$, $d_2 = 0.08$, $\beta = 1.52$ and initial condition: $u_0(x) = u_1 + 0.01\sin(x)$, $v_0(x) = v_1 + 0.2\sin(x)$. Here $\beta = 1.52$, which is near the Hopf bifurcation value $\beta = 1.50$. Hopf bifurcation occurs resulting a stable periodic solution.

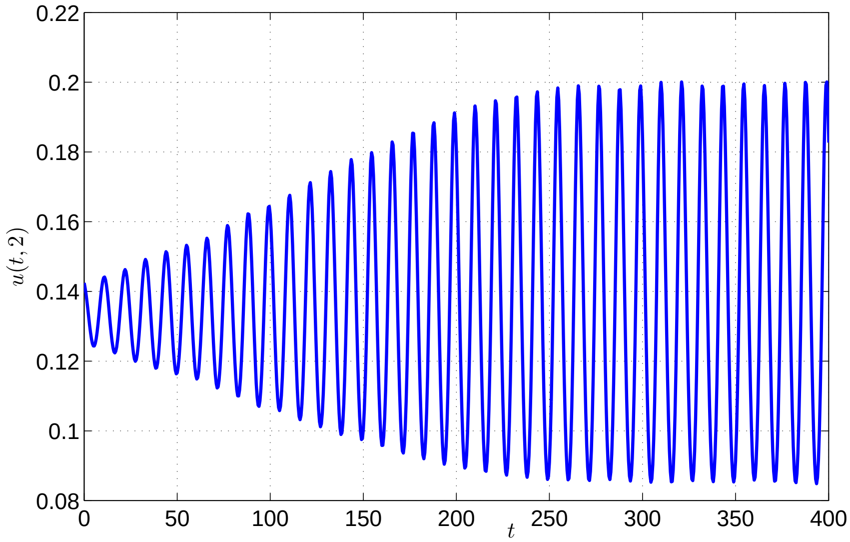

FIGURE 6. A numerical solution of System (7) with parameter values: $r = 8$, $\kappa = 0.08$, $\sigma = 5$, $d_1 = 0.008$, $d_2 = 0.08$, $\beta = 1.52$ and initial condition: $u_0(x) = u_1 + 0.01 \sin(x)$, $v_0(x) = v_1 + 0.2 \sin(x)$. Here we plot $u(t, x)$ at location $x = 2$.

interesting transient dynamics: as shown in Figures 7 and 8, if the initial distribution is of $u_0(x) = u_1 + \epsilon_1 \sin(4x), v_0(x) = v_1 + \epsilon_2 \sin(4x)$, where ϵ_1 and ϵ_2 are small real numbers, then the solution of System (7) follows around the bifurcated steady state with the wave number $n = 4$ for a short time period before it converges to a stable periodic solution.

With parameter set (ii), (14) and (23) hold, there are 8 Hopf bifurcation values $\{1.49, 1.88, 2.62, 3.87, 6.02, 10.08, 19.76, 67.27\}$, and there are no steady state bifurcation values (see Figure 9). Combining Theorems 3.6, 3.9 and 3.10, we conclude that the spatially homogeneous steady state E^* is stable if $\beta \in (0, 1.49)$ and becomes unstable if $\beta > 1.49$, there are spatially nonhomogeneous periodic solutions bifurcating from E^* when β is near the Hopf bifurcation values. Take $\beta = 1.51$, which is near the Hopf bifurcation value $\beta_1^H = 1.49$. As shown in Figure 10, a stable periodic solution bifurcates from the steady state E^* resulting oscillations.

Take $\beta = 1.89$, which is near the Hopf bifurcation value $\beta_2^H = 1.88$. For solutions with initial conditions near the bifurcated spatially non-homogeneous periodic solution with small amplitude, they undergo transient oscillations for a short time period and then evolve to a stable periodic solution with a larger amplitude. This is shown in Figure 11, where only the $u(t, x)$ is plotted and the $v(t, x)$ component behaves similarly.

With parameter set (iii), (15) and (22) hold, and there is one steady state bifurcation value $\beta_1^S = 15.60$ and there is no Hopf bifurcation value. Combining Theorems 3.6, 3.9 and 3.10, we conclude that the spatially homogeneous steady state E^* is stable if $\beta \in (0, 15.60)$ and becomes unstable if $\beta > 15.60$ and there are spatially nonhomogeneous steady states from E^* when β is near the bifurcation value. Choosing $\beta = 15.61$, our numerical simulations confirm that the spatially

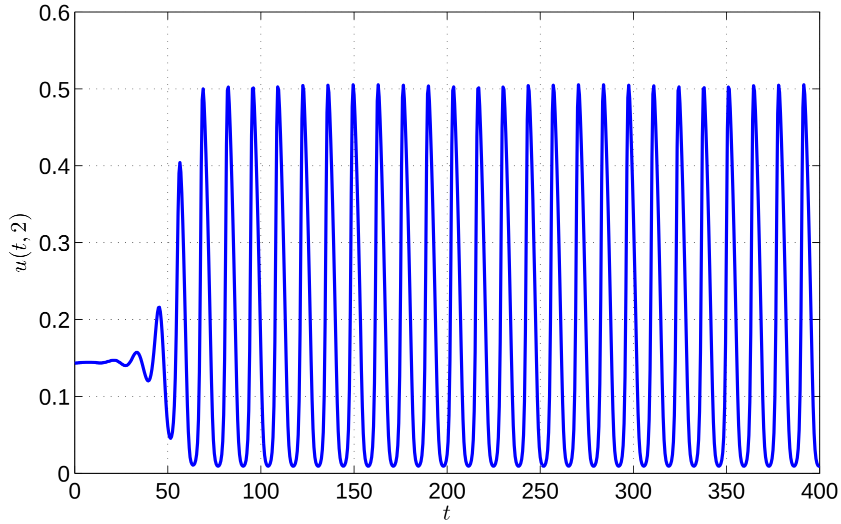

FIGURE 7. A numerical solution of System (7) with parameter values: $r = 8$, $\kappa = 0.08$, $\sigma = 5$, $d_1 = 0.008$, $d_2 = 0.08$, $\beta = 2.0$ and initial condition: $u_0(x) = u_1 + 0.01\sin(4x)$, $v_0(x) = v_1 + 0.2\sin(4x)$. Here we plot $u(t, x)$ at location $x = 2$.

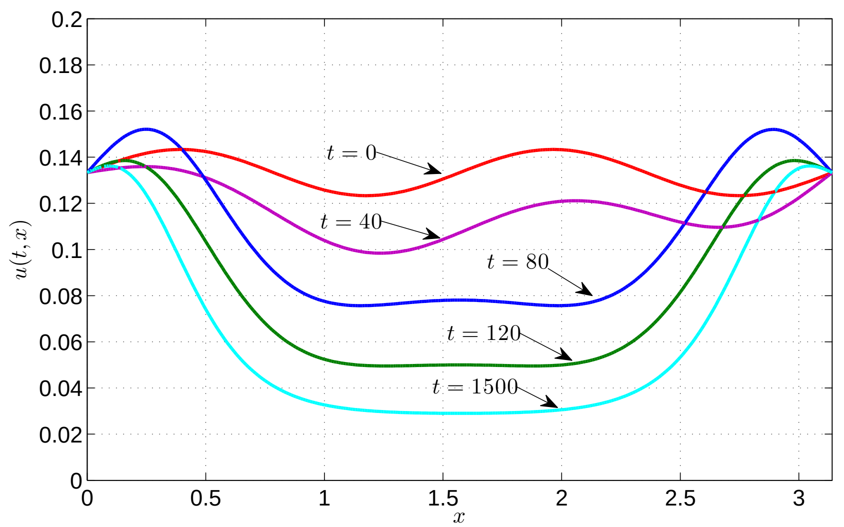

FIGURE 8. The spatial distributions of u at various times. Parameter values: $r = 8$, $\kappa = 0.08$, $\sigma = 5$, $d_1 = 0.008$, $d_2 = 0.08$, $\beta = 2.0$ and initial condition: $u_0(x) = u_1 + 0.01\sin(4x)$, $v_0(x) = v_1 + 0.2\sin(4x)$.

homogeneous steady state E^* becomes unstable. Moreover, simulations suggest that there are two spatially nonhomogeneous steady states, and both are stable. That is, a supercritical pitch-fork bifurcation occurs. For example, the solution with initial condition $u_0(x) = u_1 + 0.01\sin(x)$, $v_0(x) = v_1 + 0.2\sin(x)$ converges to

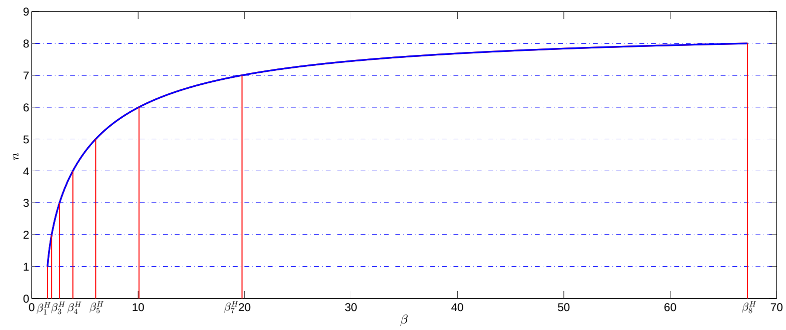

FIGURE 9. Determination of Hopf bifurcation values for System (7). Parameter values used: $r = 8$, $\kappa = 0.08$, $\sigma = 5$, $d_1 = 0.008$, $d_2 = 0.08$. Hopf bifurcation values are 1.49, 1.88, 2.62, 3.87, 6.02, 10.08, 19.76, 67.27.

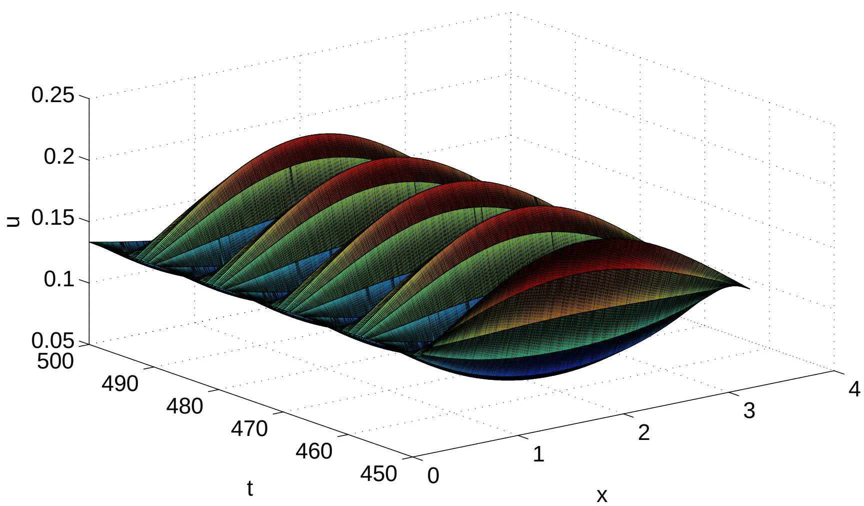

FIGURE 10. The $u-$component of a numerical solution of System (7) with parameter values: $r = 8$, $\kappa = 0.08$, $\sigma = 5$, $d_1 = 0.08$, $d_2 = 0.0008$, $\beta = 1.51$ and initial condition: $u_0(x) = u_1 + 0.01\sin(x)$, $v_0(x) = v_1 + 0.2\sin(x)$. Since $\beta = 1.51$ is near the Hopf bifurcation value $\beta_1^H = 1.49$, a stable periodic solution bifurcates from the steady state E^*.

one spatially nonhomogeneous steady state (see Figure 12 for the $u-$component of the numerical solution, where the transient dynamics is omitted and see Figure 13 for the steady state profiles), while the solution with $u_0(x) = u_1 + 0.01\sin(x)$, $v_0(x) = v_1 + 0.18\sin(x)$ converges to another spatially nonhomogeneous steady state (see Figures 14 and 15).

A bifurcation diagram is sketched in Figure 16, where we plotted the steady state distributions at location $x = 3$ against the bifurcation parameter β. As β crosses the steady state bifurcation value $\beta_1^S = 15.60$, two (stable) spatially nonhomogeneous

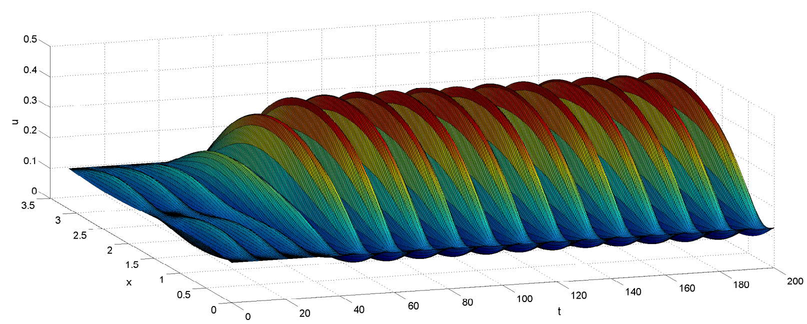

FIGURE 11. A numerical solution (the u-component) of System (7) with parameter values: $r = 8$, $\kappa = 0.08$, $\sigma = 5$, $d_1 = 0.08$, $d_2 = 0.0008$, $\beta = 1.89$ and initial condition: $u_0(x) = u_1 + 0.01\sin(2x)$, $v_0(x) = v_1 + 0.2\sin(2x)$. Since $\beta = 1.89$ is near the Hopf bifurcation value $\beta_2^H = 1.88$, the solution follows the bifurcated spatially non-homogeneous periodic solution with small amplitude for a short time period and then evolves to a stable periodic solution with a larger amplitude.

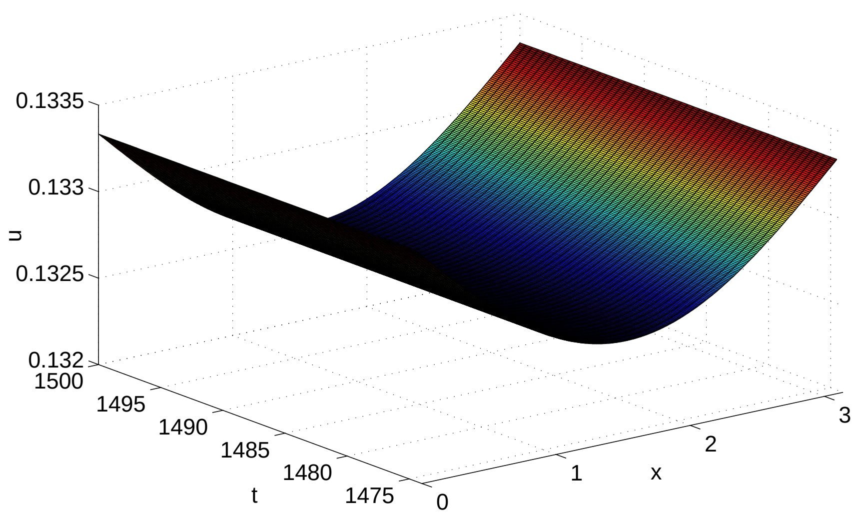

FIGURE 12. The $u-$component of a numerical solution of System (7) with parameter values: $r = 0.2$, $\kappa = 0.08$, $d_1 = 0.08$, $d_2 = 0.8$, $\sigma = 5$, $\beta = 15.61$ and initial condition: $u_0(x) = u_1 + 0.01\sin(x)$, $v_0(x) = v_1 + 0.2\sin(x)$.

steady states bifurcate from the unstable spatially homogeneous steady state E^*, indicating a supercritical pitch-fork bifurcation.

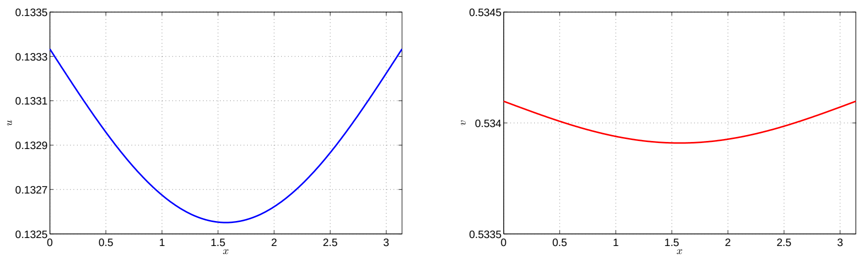

FIGURE 13. The profiles of bifurcated spatially non-homogeneous steady state of System (7) with parameter values: $r = 0.2$, $\kappa = 0.08$, $d_1 = 0.08$, $d_2 = 0.8$, $\sigma = 5$, $\beta = 15.61$ and initial condition: $u_0(x) = u_1 + 0.01\sin(x)$, $v_0(x) = v_1 + 0.2\sin(x)$.

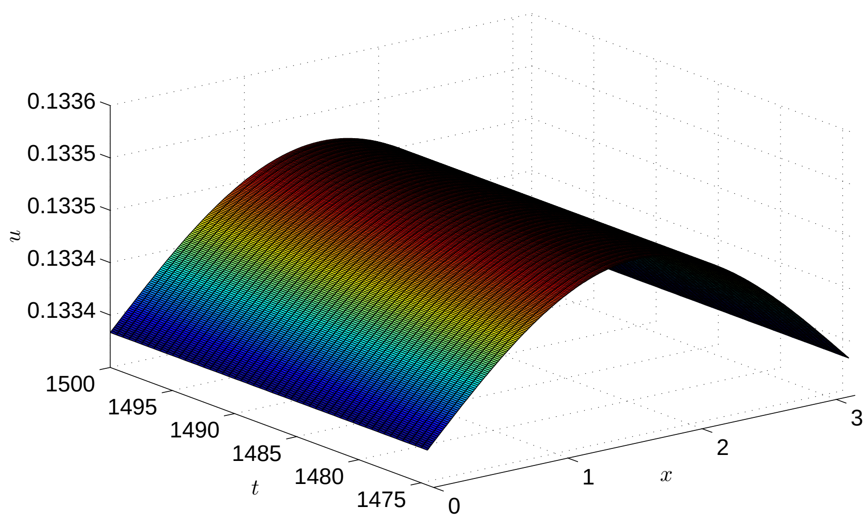

FIGURE 14. The u-component of a numerical solution of System (7) with parameter values: $r = 0.2$, $\kappa = 0.08$, $d_1 = 0.08$, $d_2 = 0.8$, $\sigma = 5$, $\beta = 15.61$ and initial condition: $u_0(x) = u_1 + 0.01\sin(x)$, $v_0(x) = v_1 + 0.18\sin(x)$.

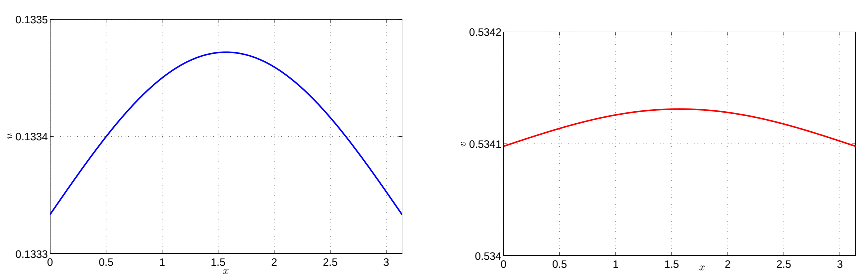

FIGURE 15. The profiles of bifurcated spatially nonhomogeneous steady state of System (7) with parameter values: $r = 0.2$, $\kappa = 0.08$, $d_1 = 0.08$, $d_2 = 0.8$, $\sigma = 5$, $\beta = 15.61$ and initial condition: $u_0(x) = u_1 + 0.01\sin(x)$, $v_0(x) = v_1 + 0.18\sin(x)$.

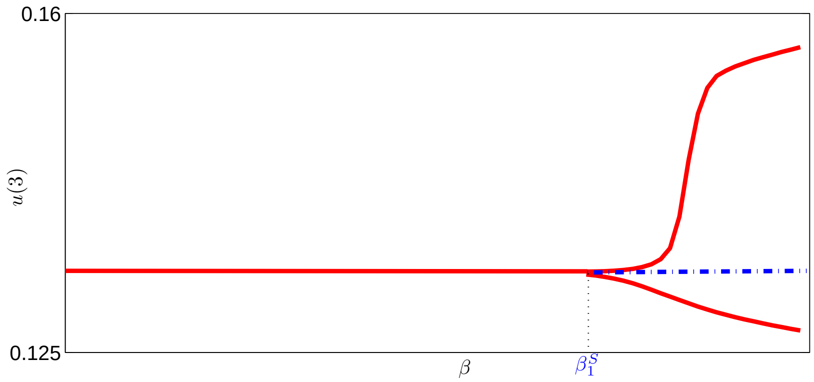

FIGURE 16. Bifurcation diagram of System (7) with parameters $r = 0.2$, $\kappa = 0.08$, $d_1 = 0.08$, $d_2 = 0.8$ and $\sigma = 5$. Here the steady state distributions at location $x = 3$ are plotted against the bifurcation parameter β.

5. **Summary and discussion.** In this paper we have considered a diffusive plant-herbivore model subject to nonzero Dirichlet boundary conditions in which the numerical response is not necessarily proportional to the functional response. For the spatially homogeneous steady state E^*, we have derived conditions under which E^* is locally stable. We have also obtained conditions under which E^* becomes unstable through a positive real root or a pair of conjugate complex roots of the characteristic equation. When E^* becomes unstable, we have shown that either (i) both Hopf bifurcations and steady state bifurcations can occur, or (ii) only Hopf bifurcations occur or (iii) only steady state bifurcations occur. For case (i), besides solutions that evolve quickly to a stable periodic solution (Figure 6), some interesting transient dynamics is also observed: there are solutions that follow a spatially nonhomogeneous steady state solution for a short time period before emerging to a stable periodic solution (Figure 7). For case (ii), transient dynamics is observed in a different manner: there are solutions that follow unstable spatially nonhomogeneous periodic solutions with small amplitudes for a short time period before emerging to a stable periodic solution with larger amplitude (Figure 11). For case (iii), as the bifurcation parameter β crosses the steady state bifurcation value, we have observed a supercritical pitch-fork bifurcation of steady states: two spatially nonhomogeneous steady states emerge and initial condition dependent bistability occurs.

Keep all other parameters and vary β. As seen from our simulations, as β increases, the steady state E^* may change from being stable to becoming unstable, and spatially nonhomogeneous steady states or spatially nonhomogeneous periodic solutions may appear. In this sense, β has a destabilizing effect. This suggests that the assumption that the numerical response is not proportional to functional response does bring in different dynamics for the plant-herbivore interactions.

Certainly diffusion in the diffusive model can stabilize the spatially homogeneous steady state, which is rather unstable in the local system without diffusion. In addition, varying the ratio of d_1/d_2 and the magnitude of d_1 and d_2 can induce the above mentioned three possible scenarios. This indicates that the diffusion also has impact on the dynamics of the plant-herbivore interactions. We point out that transient oscillatory patterns were recently explored in [11] for the diffusive non-local blowfly equation with delay under the zero-flux boundary condition, in which the transient dynamics are mainly driven by the time delay, it is very interesting to incorporate time delay into our model and study the joint effects of time delay and the diffusion on the transient dynamics. We leave this for our future project.

Acknowledgments. The authors would like to thank the anonymous reviewer for his/her very helpful comments and suggestions.

REFERENCES

[1] J. Blat and K. J. Brown, Global bifurcation of positive solutions in some system of elliptic equations, *SIAM J. Math. Anal.*, **17** (1986), 1339–1353.
[2] E. Conway, R. Gardner and J. Smoller, Stability and bifurcation of steady-state solutions for predator-prey equations, *Adv. in Appl. Math.*, **3** (1982), 288–334.
[3] M. G. Crandall and P. H. Rabinowitz, Bifurcation from simple eigenvalues, *J. Funct. Anal.*, **8** (1971), 321–340.
[4] E. N. Dancer, On positive solutions of some pairs of differential equations, *Trans. Amer. Math. Soc.*, **284** (1984), 729–743.
[5] E. N. Dancer, On positive solutions of some pairs of differential equations II, *J. Diff. Equat.*, **60** (1985), 236–258.
[6] L. R. Fox, Defense and dynamics in plant-herbivore systems, *Amer. Zool.*, **21** (1981), 853–864.
[7] B. D. Hassard, N. D. KazavinoJ and Y. H. Wan, *Theory and Applications of the Hopf Bifurcation*, Cambridge University Press, Cambridge, MA, 1981.
[8] L. R. Ginzburg, Assuming reproduction to be a function of consumption raises doubts about some popular predator–prey models, *J. of Animal Ecology*, **67** (1998), 325–327.
[9] L. Li, Coexistence theorems of steady states for predator-prey interacting systems, *Trans. Amer. Math. Soc.*, **305** (1988), 143–166.
[10] R. E. Ricklefs, *The Economy of Nature*, Freeman and Company, New York, 2010.
[11] Y. Su and X. Zou, Transient oscillatory patterns in the diffusive non-local blowfly equation with delay under the zero-flux boundary condition, *Nonlinearity*, **27** (2014), 87–104.
[12] Y. Yamada, Stability of steady states for prey-predator diffusion equations with homogeneous Dirichlet conditions, *SIAM J. Math. Anal.*, **21** (1990), 327–345.

Received March 23, 2014; Accepted December 02, 2014.

E-mail address: lwang2@unb.ca
E-mail address: watmough@unb.ca
E-mail address: yufang77@gmail.com